Molecular Docking and Simulation Studies of FDA Approved Drugs Targeting Allosteric Inhibition of Glycogen Synthase Kinase-3β

Suggala Ramya Shri[1], Yogendra Nayak[1], K Sreedhara Ranganath Pai[1,*]

[1] Department of Pharmacology, Manipal College of Pharmaceutical Sciences, Manipal Academy of Higher Education (MAHE), Manipal -576104, India

ABSTRACT

Background: Inhibition of glycogen synthase kinase (GSK-3β) by various mechanisms of inhibition has become an important drug target for treating neurodegenerative diseases such as Alzheimer's disease (AD). AD is characterized by cognitive, memory loss, and behavioral impairments. The pathological hallmarks of AD which appear before the clinical symptoms are neurofibrillary tangles and amyloid plaques.

Aim and Objectives: In the present study, we focused on the in-silico-based prediction approach for the virtual screening of FDA-approved ligands (Drug bank database) to target the allosteric pocket of GSK-3β, with the help of Schrodinger (Maestro software).

Results and Conclusion: After various levels of screening compounds, out of 2133 FDA-approved ligands, only three compounds formoterol, salmeterol, and polydatin were subjected to induced fit docking (IFD). After performing IFD, one top pose of the above three compounds was proposed for molecular dynamics studies by using the Desmond module. Formoterol showed the most stable interactions with the key amino acid residues. However, further to confirm these finding experimental studies are required.

Keywords: Alzheimer's disease; GSK-3β Molecular docking; Induced fit docking; Molecular dynamics simulations.

INTRODUCTION

Today a lot of improvements occurred in treatment aspects, diagnostic strategies, neuroimaging studies, neuropsychological testing, and brain imaging technical tools, but 44 million people are suffering from neurocognitive diseases. Currently, quite a lot of medications are being tried for Alzheimer's disease (AD), and several mechanisms arrived for the pathological treatment[1]**.** AD is a neurodegenerative disease, progressively damages the neurons, particularly the hippocampus of the brain which is responsible for memory, learning, judgment, language, and reasoning. The available treatments provide only symptomatic relief, still there is no permanent cure for AD with current therapies[2]. The available treatments focus on reducing the tau hyperphosphorylation and amyloid beta levels[3]. Protein kinases are essential for the transduction of signals required for normal cellular process. These kinases are found in almost all eukaryotic species [4]. They catalyze the transfer of a phosphate group onto a protein substrate and, because of deregulations of protein kinase, is implicated in a large variety of diseases[5]. GSK-3β is a constitutively active multifunctional serine-threonine kinase that belongs to the phosphotransferase family. It is involved in different aspects of cell physiology, such as proliferation, metabolism, and

[*]***Corresponding author: K. Sreedhara Ranganath Pai***
ksr.pai@manipal.edu
Received: 4/7/2024 Accepted: 20/2/2025.
DOI: https://doi.org/10.35516/jjps.v19i2.2906

apoptosis[6]. GSK-3 has two isoforms they are GSK-3α and GSK-3β, but GSK-3β has a constitutively active form. Kinase is phosphorylated at SER9 (inactive form) and phosphorylated at TYR216. Therefore, GSK-3β has become one of the most important therapeutic targets for these diseases [7]. A large number of GSK-3β inhibitors are available for several pathologies, but none of them finished the clinical trials and entered the market within the proposed time because of off-target activities and lack of inhibitor activity [8]. The goal of non-ATP GSK-3β competitive inhibitors can bind to a particle protein of interest reference binding site. The allosteric GSK-3β inhibitors can bind the particle region of the protein with high selectivity, but for identification of allosteric druggable site [9,10]. In allosteric inhibition, the inhibitor binds to a distant site away from the active site, rendering the active site unfit for the substrate to bind[11]. Tideglusib, a small thiadiazolidindione (TDZD) family, is the first non-ATP competitive GSK-3β inhibitor and in different neurodegenerative models, this tideglusib has shown neuroprotective activity and anti-inflammatory activity also[12,13]**.** Tideglusib and VP0.7 treatment didn't produce an elevated level of phosphorylation of SER9 (GSK-3β) in LGMDR1 (Limb-girdle muscular dystrophy R1 calpain 3-related) patients and fibroblasts of controls patients. Since this indicates that these two inhibitors belong to allosteric GSK-3β [14]. Similarly, Allosteric modulators of protein kinases are likely to be more selective, less information is available on *in-vitro* studies and this provides a rationale for comprehending and anticipating the effects of an Allosteric GSK-3β inhibitor with GSK-3β enzyme. In this study, we used an in-silico approach to screen the FDA-approved ligands (drug bank database) against GSK-3β (1PYX).

COMPUTATIONAL METHODOLOGY

Retrieval and preparation of receptor

The structural coordinates for GSK-3β (PDB ID: 1PYX) were acquired from the RCSB Protein Data Bank (Research Collaboratory for Structural Bioinformatics) [15]. The protein structure was processed using Schrodinger software's Protein Preparation Wizard. Initially, bond ordering for untemplated residues were estimated, and explicit hydrogens were included into the structure. To solve missing structural parts, a Prime task was used to fill up loops and side chains. This procedure involved examining the immediate surroundings of the missing areas, which included neighboring residues and their spatial conformations. The Prime approach predicts the best conformations for these missing segments by energy reduction techniques. Specifically, loops from SER119 to GLU126 and PRO286 to PHE291 were planned for completion. In addition, bonds between sulfur atoms were formed, and missing side chain atoms were inserted and optimized. To simplify the structure, water molecules larger than 5.0 Å were removed from heteroatoms and ions. Water orientations were collected during hydrogen bond assignment to ensure that water molecules were properly positioned relative to protein residues and that hydrogen bonding interactions were effective. Protonation states of ionizable residues were improved using PROPKA at pH 7. Water molecules larger than 3.0 Å from any heteroatom were also excluded. Restrained minimization was used to optimize non-hydrogen atom locations, resulting in constant alignment within 0.30 Å of starting structural coordinates [16]. These comprehensive processes ensured that the optimized protein structure is ready for molecular docking, molecular dynamics simulations providing a foundation for studying protein-ligand interactions.

Retrieval and preparation of ligands

This study's computational tests used FDA-approved pharmaceuticals from the Drug Bank database, which included 2133 ligands. Prior to molecular docking with the target protein, these ligands were thoroughly prepared using the LigPrep tool in the Schrödinger Suite. LigPrep makes it easier to generate a wide range of ligand conformations and ionization states, which is required for accurate docking simulation. The Epik tool inside LigPrep was used to compute all possible ionization states throughout a pH range of 7 ± 2, and generate tautomers for each neutralized or ionized molecule. This technique verified that the ligands' input 3D geometries correctly determined atom chiralities, resulting in the production of up to 32 unique chiral structures per ligand depending on their geometric features. Following this preliminary step, the ligands were adjusted with the OPLS3e force field to ensure that they were in an energetically favorable condition for future docking investigations. The optimized structures were stored in Maestro format, allowing for further investigation and docking against GSK-3β. Furthermore, the LigPrep settings included assigning suitable charges depending on the relevant ambient pH values for this investigation, ensuring that the ligands' protonation statuses were accurately evaluated based on their chemical characteristics. The charge assignment was confirmed by reviewing the LigPrep output files, which showed that the charges matched the predicted values for each ligand. Following this preliminary step, the ligands were adjusted with the OPLS3e force field to guarantee they were in an energetically favorable condition for future docking investigations. The optimal structures were stored in Maestro format, ready for further investigation and docking with GSK-3β.

SiteMap preparation and evaluation

1PYX structure coordinate contains two chains, chain A and chain B, but chain B and co-bonded **(Phosphoaminophosphonic acid-adenylate ester)** was removed from the crystal structure, retaining only chain A. SiteMap in Schrodinger software was used to identify the predicted binding pockets on the surface of protein for ligand binding. It reports seven pockets, requires at least 15 amino acids per each reported pocket, more restrictive definition of hydrophobicity, with a standard grid and without any detect shallow binding site inside the protein of interest. The SiteMap provides information related to the druggability of the detectable protein and visualizes the pockets[17]. Sitemap analysis revealed the presence of seven pockets with good site scores and D scores. Selecting binding sites for molecular docking experiments is critical in allosteric inhibition of GSK-3β. Pocket-7 was identified as a viable drug-binding site in a recent study on exploring the Binding Sites of Glycogen Synthase Kinase 3, Identification and Characterization of Allosteric Modulation Cavities [18]. Its unique composition and structural characteristics make it especially significant. This pocket contains important residues such as HIS173, CYS178, LEU207, ARG209, GLU211, THR235, THER330, TYR234, SER236, and SER369, which play critical roles in stabilizing ligand contacts and promoting conformational changes required for allosteric regulation. The presence of arginine (ARG 209) implies possible electrostatic interactions that might increase binding affinity, whilst serine (SER 236) and threonine (THR 235 and THR 330) offer hydroxyl groups that can form hydrogen bonds with ligands. This was demonstrated by the creation of a π-cation contact between Arg209 and the aromatic ring of the inhibitor VP0.7, as well as a

hydrophobic interaction between the methyl group of the inhibitor VP0.7 and the amino acid residue Thr235. Additionally, proline (PRO 331) adds to the structural stiffness of the pocket, which may influence ligand orientation and binding kinetics. A hydrogen bond is formed between the oxygen of the inhibitor VP0.7 and the backbone NH group of the SER236 amino acid residue. Finally, the aliphatic chain of the inhibitor VP0.7 was expanded around the hydrophobic area defined by Leu169, Pro331, and Thr330. Understanding these interactions not only helps in the rational design of FDA-approved medications that target this allosteric region, but it also improves the prediction ability of molecular docking simulations. Our computational investigations focused on pocket-7, an allosteric binding pocket, to improve therapeutic options for modulating GSK-3β activity. Grid was generated using the coordinates of pocket-7 as identified by the SiteMap tool.

Ligand docking studies

The GSK-3β structure (human) consists of 433 amino acid sequences lengthwise and 48,034 mass (Da) [8]. Whereas the GSK-3β protein structure consists of a C-terminal with the α-helical domain it contains residues from 136 to 343 and an N-terminal with β-strand domains, it contains amino acid from 25 to 138 also contain many antiparallel strands[19]. The ligand were docked to the receptor grid that contained the amino acid residues for allosteric inhibition of GSK-3β, as described by Palomo et al. who covered seven pockets using fpocket software, among which one pocket is allosteric, and the remaining pockets being ATP competitive site (orthosteric site), substrate binding pocket, and Axin/ FRAT tide binding site respectively. The findings are reproduced in the Table 1 [20,21]. GLIDE was used to dock the prepared FDA-approved compounds to the pocket on the GSK-3β surface. Before ligand docking the receptor grid was generated [22] in the workspace with a ligand you must identify the ligand molecule so it can be excluded from the grid generation, then pick the ligand entry with showed markers. Whereas the endosing box the docked ligand is confined to the endorsing box center centroid of the workspace ligand, the dock ligands are similar in size to the workspace ligand. Then after grid generation, browse that file for the ligand to be docked from the workspace was selected. Here we subjected the ligands to a flexible docking setting, including non-ring nitrogen inversions during conformer generation and sample ring conformations using a template during conformer generation, the biased sampling for the torsions defined with a bias type in the resource file, with added Epik state penalties to the docking score. The file type writes the receptor and ligand poses to the structure file, several poses per ligand to be included is five. For post-docking minimization, compute the RMS deviation against the input ligand geometry of each ligand. Finally, results have been analyzed based on molecular interactions and docking scores.

Molecular Dynamics Simulations

The protein-ligand complex was selected and the first step is to build the system by using a system builder module with predefined TIP3P solvent model under periodic boundary conditions are orthorhombic shape box with dimensions of 10.0*10.0*10.0. The system required Na^+/Cl^- ions to be added to neutralize by maintaining the salt concentration of 0.15M. After the system builder subjected it to minimization to relax the model system with a local energy minimization simulation time total of 100.0ps. Then minimized file was loaded for continuing

the molecular dynamics model system simulation with a simulation time total of 100 ns, energy is 1.2, recording interval trajectory 100.0 ps with 1000 number of the approximate number of frames using NPT ensemble class, pressure 1.01325, the temperature is 300K and finally relax the model system before simulation[23,24].

RESULTS AND DISCUSSION

Protein structure

Binding site accessibility and conformational flexibility are critical factors in the study of GSK-3β, particularly when developing allosteric inhibitors. The structure designated as 1PYX not only provides detailed insights into potential binding pockets but also demonstrates significant conformational changes upon ligand interaction, which are essential for understanding allosteric modulation. Research utilizing 1PYX has underscored its potential in designing selective allosteric modulators capable of fine-tuning GSK-3β activity while maintaining physiological functions. This aligns with the growing focus on allosteric modulation, given the high homology of ATP-binding sites across kinases, which can lead to undesirable off-target effects. Consequently, 1PYX enables exploration of novel binding interactions and mechanisms of various small molecules [14,25,26].

Drug binding site prediction with SiteMap

As 1PYX protein was co-crystalized with an orthosteric ligand, our target of interest is allosteric. So for the prediction of the allosteric drug binding site, we used the SiteMap tool. From SiteMap results we can know the druggable site score, Dscore, donor/acceptor region, volume, hydrophobic region, hydrophilic regions and residues of our respective protein.

Site-2 represented as Allosteric site here with had a site score, Dscore, volume, hydrophobic region and the hydrophilic regions of 0.952, 0.978, and 271.999 $Å^3$, 0.338 $Å^2$, and 0.975 $Å^2$ respectively. The findings of aminoacid residues in the binding pocket were in consist with the findings of the martin. The site 2 contained amino acid residues of ALA170, HIS173, SER174, LEU207, VAL208, ARG209, GLY210, GLU211, PRO212, ASN213, GLU226, ALA231, THR232, ASP233, TYR234, THR235, SER236, SER237, ILE238, VAL240, GLU283, MET284, ASN285, ARG319, PRO325, THR326, ALA327, ARG328, THR330, PRO331, LEU332, GLN365, GLU366, SER368, SER369. Consequently, the for Site-1, had a site score, D score of is 1.006, and 0.89, respectively with donor/acceptor region for Site-1 is 0.356 $Å^2$, volume, and area for hydrophobic and hydrophilic to be 506.954 $Å^3$, 0.401 $Å^2$, and 1.456 $Å^2$ respectively. Site-3, had a site score, D score of is 0.722, 0.681, respectively with donor/acceptor region for Site-3 is 1.465 $Å^2$, volume, and area for hydrophobic and hydrophilic to be 111.132 $Å^3$, 0.592 $Å^2$, and 0.902 $Å^2$. Site-4, had a site score, D score of is 0.623, 0.59, respectively with donor/acceptor region for Site-4 is 0.490$Å^2$, volume, and area for hydrophobic and hydrophilic to be 101.528 $Å^3$, 0.440 $Å^2$, and 0.805 $Å^2$. Site-5, had a site score, D score of is 0.657, 0.602, respectively with donor/acceptor region for Site-5 is 2.520 $Å^2$, volume, and area for hydrophobic and hydrophilic to be 60.368 $Å^3$, 0.495 $Å^2$, and 0.855 $Å^2$. The residue related to each site is listed in Figure 1.The finding of various amino acid residues and their designation as ATP-binding site and allosteric sites based on the findings of Martin, who also observed the presence of same amino acid residue in their binding pocket. The findings of sitemap, including the identification of seven potential ligand binding sites, their sitescore, dscore, volumes and the amino acid resudues are illustrated in Table 1. The druggable score value between 0.5 and 1.0 was consider the pocket as

druggable and druggable score closer to 1 are considered the best. druggable Dscore are grouped into four main classes they are 1. Very druggable Dscore value 1, druggable Dscore value range is 0.75 and <1, moderate druggable Dscore value range is 0.50 and <0.75 and difficult Dscore value range is <0.5[27]. In the current research we have generated the receptor glide grid at the Site-2 encompassing amino acid residues ALA170, HIS173, SER174, LEU207, VAL208, ARG209, GLY210, GLU211, PRO212, ASN213, GLU226, ALA231, THR232, ASP233, TYR234, THR235, SER236, SER237, ILE238, VAL240, GLU283, MET284, ASN285, ARG319, PRO325, THR326, ALA327, ARG328, THR330, PRO331, LEU332, GLN365, GLU366, SER368, SER369, all these residues are essential for the allosteric targeting inhibition of GSK-3β. Based on Valle Palmo et al. used the fpocket program to study the GSK-3 surface, the main aim of their study is to identify the possible allosteric binding pockets. At least seven pockets were found in all 25 GSK-3 ligand complexed PDBs. The amino acids involved, detailed description, and validation of each pocket on the GSK-3 surface were carried out by the fpocket program. The pocket 1 corresponds to ATP competitive GSK-3β binding inhibitor with residues ASP200, LEU188, ASN186, ASP113, VAL135, TYR134, CYS199, GLU97, THR138, and LYS85. The pocket 2 corresponds to substrate binding site of GSK-3β with residues LYS94, ASN95, ARG180, GLU97, ARG96, PHE67, PHE93, LYS205, and GLN89. Pocket 3 corresponds to the axin/fratide binding site of GSK-3β with residues ARG220, SER215, PHE229, and ARG223. Pocket 4 with residues ARG144, ARG220, GLU249, SER219, GLN185, ARG148, TYR221, TYR140, and TYR222. Pocket 5 with residues TYR56, TYR71, THR38, LYS86, MET26, and SER119. Pocket 6 with residues ARG111, ASP133, VAL135, LYS197, ASP190, GLU80, and ARG113. The pocket 7 corresponds to allosteric binding site of GSK-3β with residues CYS178, GLU211, THR235, ARG209, LEU207, HIS173, TYR234, SER369, THER330, and SER236. All 25 GSK-3 ligand complexed PDB structures were aligned by using a max cluster and visually inspected at the P-loop region. Based on P-loop conformations Valle Palomo et al. selected three GSK-3β ligand complexed PDB structures they are 1Q41, 1Q4L, and 1PYX. Among three GSK-3β ligand complexed PDB they have selected 1PYX for studying[28]. Our SiteMap analysis showed 4 additional binding sites or pockets with good number druggable site score, Dscore, donor/acceptor region, volume, hydrophobic region, hydrophilic regions and residues but all those belongs to different binding targets.

Table 1: The binding pockets of 1PYX along with their Site score and residues

Name	Site score	D score	donor/acceptor region	Volume ($Å^3$)	Hydrophobic region ($Å^2$)	Hydrophilic regions ($Å^2$)	Residues
ATP-competitive binding pocket or Site 1	1.006	0.89	0.356	506.954	0.401	1.456	Chain A: ILE62,GLY63,ASN64,GLY65, SER66,PHE67,GLY68,VAL70, ALA83,LYS85,VAL87,LEU88, GLN89,ASP90,LYS94,ASN95, ARG96,GLU97,MET101,VAL 110,LEU132,TYR134,VAL135, PRO136,GLU137,THR138,TY R140,ARG141,ARG180,ASP18 1,LYS183,GLN185,ASN186,L EU188,CYS199,ASP200,PHE2 01,GLY202,SER203,ALA204,1 002,1003
Allosteric binding pocket or Site 2	0.952	0.978	1.316	271.999	0.338	0.975	Chain A: ALA170,HIS173,SER174,LEU 207,VAL208,ARG209,GLY210 ,GLU211,PRO212,ASN213,GL U226,ALA231,THR232, ASP233, TYR234, THR235, SER236, SER237, ILE238, VAL240, GLU283, MET284, ASN285, ARG319, PRO325, THR326, ALA327, ARG328, THR330, PRO331, LEU332, GLN365, GLU366, SER368, SER369
Pocket -3 or Site 3	0.722	0.681	1.465	111.132	0.592	0.902	Chain A: TYR140,ALA143,ARG144,SE R147,ARG148,GLN185,ARG2 20,TYR221,TYR222,GLU249, GLY253,GLN254,PRO255
Pocket -4 or Site 4	0.623	0.59	0.490	101.528	0.440	0.805	Chain A: SER35,LYS36,THR38,TYR56, THR57,ASP58,THR59,TYR71, ILE84,LYS86,PHE116,SER118 ,ASN129
Pocket -5 or Site 5	0.657	0.602	2.520	60.368	0.495	0.855	Chain A: GLN151,THR152,LEU153,VA L155,VAL158,LEU250,LEU25 1,LEU252,PHE305,ARG306,T HR309,PRO310

Figure 1: Various Pockets of 1PYX

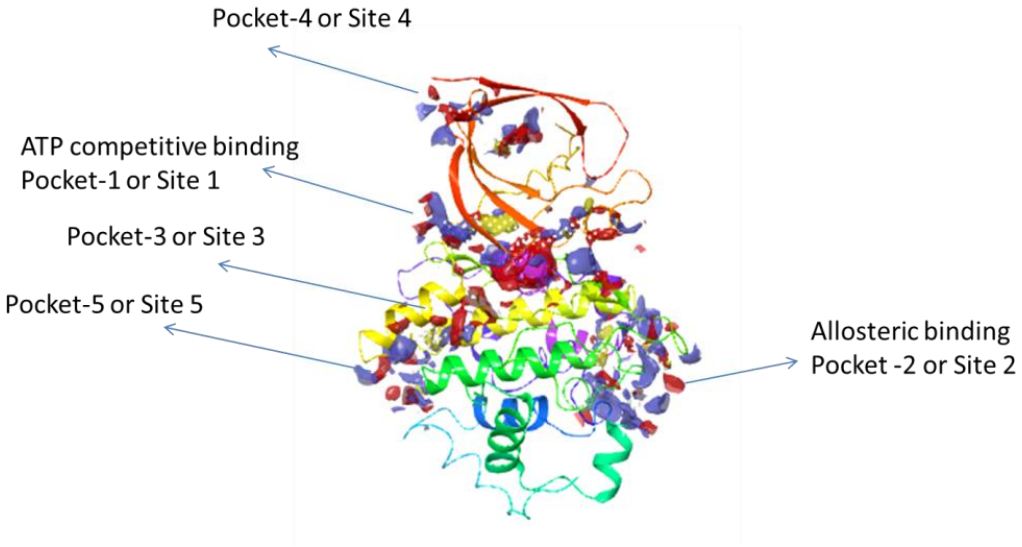

Figure 1 caption: Illustration of different Sites of (1PYX) protein and the position of various pockets are clearly showed in this figure.

Ligand docking studies

The non-ATP competitive GSK-3β inhibitors show distinct pharmacological advantages. A variety of allosteric modulators have been reported and identified. Some of those inhibitors are listed here 1. Tideglusib is one of the non-ATP competitive GSK-3β inhibitors, the treatment with tideglusib showed improved cognitive deficits in transgenic mice and also reduced the tau phosphorylation in human neuroblastoma cells [29,30]. 2. Benzothiazinones (BTO-5h) is a GSK-3β allosteric inhibitor. 1pyx (GSK-3β) crystal structure was used and mentioned ARG209, and ASP233 amino acids have formed an interaction with hydrogen bonds that played a prominent key role in allosteric modulation. The binding of ARG209, THR235, and SER236 in the allosteric pocket has been related to the active conformation of the GSK-3β enzyme [31] [32]. 3. Valle Palomo et al. generated a grid based on previously identified pocket 7 in the GSK-3β (1PYX). The compound 1(Quinoline moiety) formed an interaction with ARG209 which is located in the 1PYX activation loop region and another interaction is formed with SER236. The hydrophobic region of the pocket contains residues such as THR330, ARG328, and PRO331 which are produced mainly by hydrophobic interaction between the aliphatic chain region of the inhibitor[33].

In the present study to predict the drug binding of the prepared FDA _approved compounds to the pocket on the 1PYX (GSK-3β) enzyme surface, whereas the GSK-3β enzyme belongs to the serine/threonine family

of kinases. Here we have used the x-ray diffraction crystal structure with a resolution of 2.40Å for ligand docking studies. The GSK-3β consists of mainly four parts the N-terminal domain, C-terminal domain, Hinge region, and Activation loop region. The 1PYX inbounded co-crystal structure is present at the hinge region and is also categorized as an ATP-competitive binding site, but our main target is Allosteric. So we used the SiteMap tool. From SiteMap results we came to know the Allosteric drug binding site of 1PYX. Then we docked all prepared FDA _approved ligands to the Allosteric binding pocket or Site 2 followed by the selection of top-scored (≥-5.0 kcal/mol) ligands was made based on SP docking (2013) for further XP docking. Further top 225 XP ligands with docking score (≥-7.0 kcal/mol). The GScore separates the compounds with no binding affinity to high binding affinity.

The amino moiety of the carbamonyl chain attached to pyridine ring made direct hydrogen bonding interactions with ASP233 amino acid. Similarly, the carbonyl group of the same chain made direct hydrogen bonding interactions with ARG209 amino acid. The two hydroxyl moieties in the oxolan ring that is attached to pyridine ring made direct hydrogen bonding interactions with SER236 amino acid. The phosphate moieties in the ligand made direct hydrogen bonding interactions with ARG209 and GLU206 amino acid. The hydroxyl moieties in the oxolan ring attached to purine ring made direct hydrogen bonding interactions with SER174 amino acid. The N-1 of purine ring made hydrogen bonding interactions with LYS103 amino acid as shown in NADH interaction diagram and with a docking score/XP GScore -7.815Kcal/mol.

The hydroxymethyl region of the compound showed direct hydrogen bonding interactions with HIE173. The 4-hydroxyl group in the oxane-3,4,5-triol formed direct hydrogen bonding interactions with THR235. The phenoxy ring hydroxyl group made direct hydrogen bonding interactions with SER236. The 4-hydroxyphenyl group made direct hydrogen bonding interaction with GLU211 as shown in Polydatin interaction diagram and with a docking score/XP GScore -7.351 Kcal/mol.

The 4-methoxyphenyl region of the ring showed direct hydrogen bonding interaction with SER236, the 2-aminophenol region of the ring showed direct interaction with TYR234, and the N-methyl formamide ring showed direct hydrogen bonding interaction with GLY210 as shown in Formoterol interaction diagram and with a docking score/ XP GScore -7.349 Kcal/mol.

2-(hydroxymethyl)phenol group of the ring showed direct hydrogen bonding interaction with VAL208, benzeneol ring showed direct hydrogen bonding interaction with SER236 as shown in the Salmeterol interaction diagram and with a docking score/XP GScore -7.407 Kcal/mol. The list of top XP GScore/ docking scores and non-bonded residues of all these compounds was represented in Table 2. But our main aim is to select the ligand with less cost and showing more interaction. So based on this process, we selected Salmeterol, Formoterol and Polydatin.

Table 2: Docking score of the ligands along with Interaction diagrams

S.NO	Name	Docking Score/XP Gscore	Interaction Diagram	Non-bonded interactions
1	NADH	-7.815	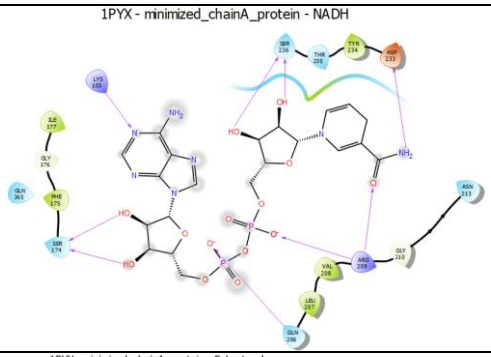	GLN365, PHE175, GLY176, ILE177, LEU207, VAL208, GLY210, ASN213, THR235, TYR234
2	Salmeterol	-7.407	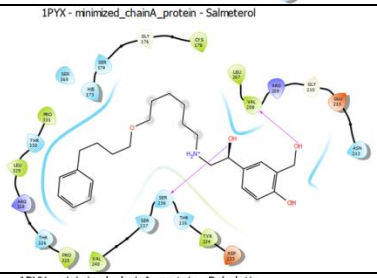	SER369, PRO331, THR330, LEU329, ARG328, THR326, PRO325, VAL240, SER237, THR235, TYR234, ASP233, ASN213, GLU211, GLY210, ARG209, LEU207, CYS178, GLY176, SER174, HIE173, SER369
3	Polydatin	-7.351	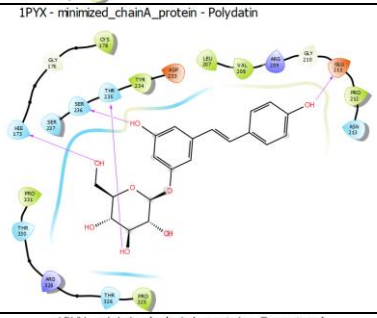	CYS178, GLY176, ASN213, PRO212, GLY210, ARG209, VAL208, LEU207, ASP233, TYR234, SER237, PRO331, THR330, ARG328, THR326, PRO325
4	Formoterol	-7.349	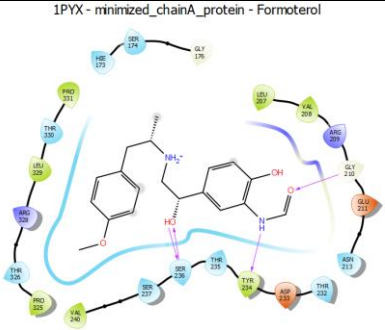	GLY176, SER174, HIE173, PRO331, THR330, LEU329, ARG328, THR326, PRO325, VAL240, SER237, THR235, ASP233, THR232, ASN213, GLU211, ARG209, VAL208, LEU207

Induced fit docking (IFD) analyses

The top 4 compounds were subjected to induced fit docking (IFD). This study was done to identify any changes in the binding of different compounds at various poses. Here we use standard precision, a maximum of 10 to 20 possible poses has been generated for each compound, among them

salmeterol, polydatin, and formoterol their top pose were listed in Table 4. The ligand interactions along with their key amino acid residues of salmeterol GLU283, SER236, and ASP233 showed a hydrogen bond interaction with the protein, and the IFD score of this pose is -698.29 Kcal/mol, similarly, the polydatin showed a hydrogen bonded interaction with SER369, GLU366, SER236, LEU207, HIE173 amino acids and one PI-PI interaction with HIE 173 with the protein and the IFD score of this pose is -699.33 Kcal/mol, and similarly the formoterol showed a hydrogen bonded interaction with SER 368, ARG328, SER 237 with the protein and its IFD score is -696.66 Kcal/mol.

Table 4: IFD poses and their interactions diagrams of the short-listed drugs

S.No	Name	IFD score	Interaction diagram	Non-bonded Interaction
1	Salmeterol	-698.29	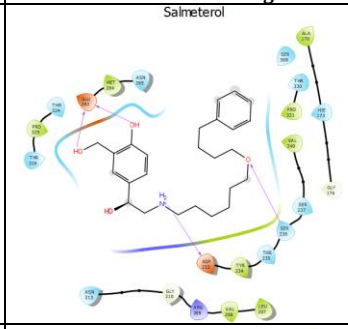	ALA170, HIE173, GLY176, SER369, THR330, PRO331, VAL240, SER237, THR235, TYR234, LEU207, VAL208, ARG209, GLY210, ASN213, ASN285, MET284, THR324, PRO325, THR326
2.	Polydatin	-699.33	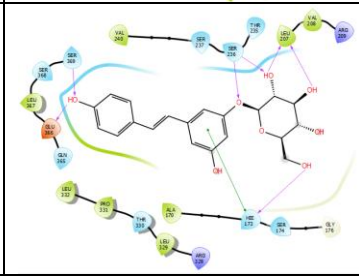	ARG209, VAL208, THR235, SER237, VAL240, SER368, LEU367, GLN365, LEU332, PRO331, THR330, LEU329, ARG328, ALA170, SER174, GLY176
3	Formoterol	-696.66	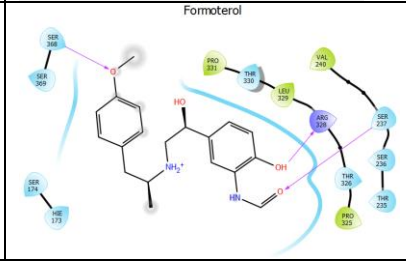	HIE173, SER174, SER369, PRO331, THR330, LEU329, THR326, PRO325, VAL240, SER236, THR235

Molecular Dynamic Simulation studies with Desmond

Molecular simulation studies are an extension of induced fit docking studies which were used to examine the protein and ligand-protein complex conformational stability in a particular duration of time nanoseconds (ns). This study provides information related to the protein-ligand interaction, RMSD variation can be assessed and RMSF fluctuation can be assessed for protein-ligand complex. The complex was then regarded stable if it fell within the 3Å range. The top-scored compounds that are selected after performing IFD studies are formoterol, salmeterol and polydatin (Figure 2, Figure 3, Figure 4, Figure 5) were subjected to Molecular dynamic simulation study using Desmond. This study was done because it mimics the physiological condition, with the help of biological significance we can predict the information related to the protein and ligand interaction.

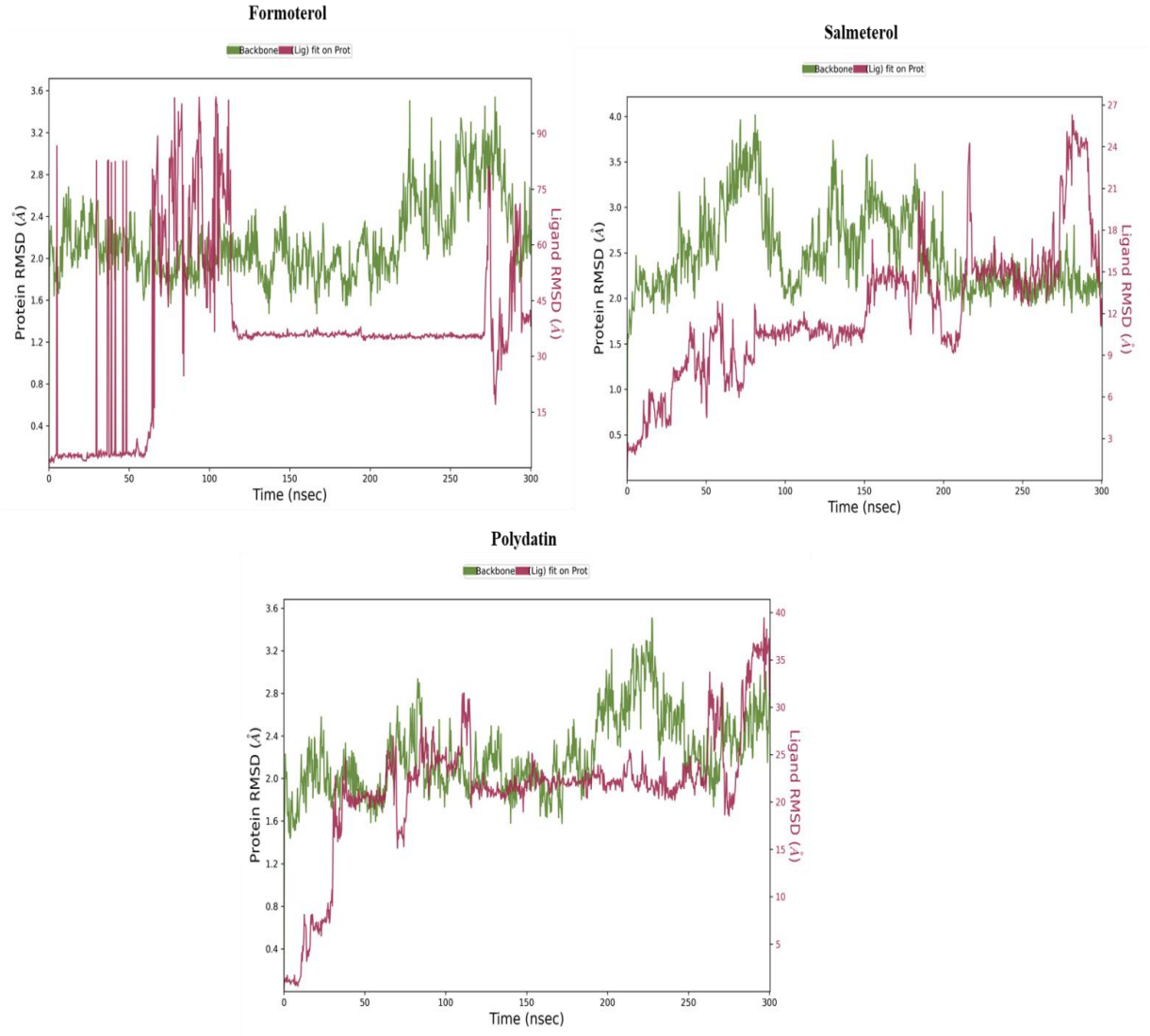

Figure 2: The RMSD observed during the MD simulation of 1PYX (protein) with ligands (Formoterol, Salmeterol and Polydatin)

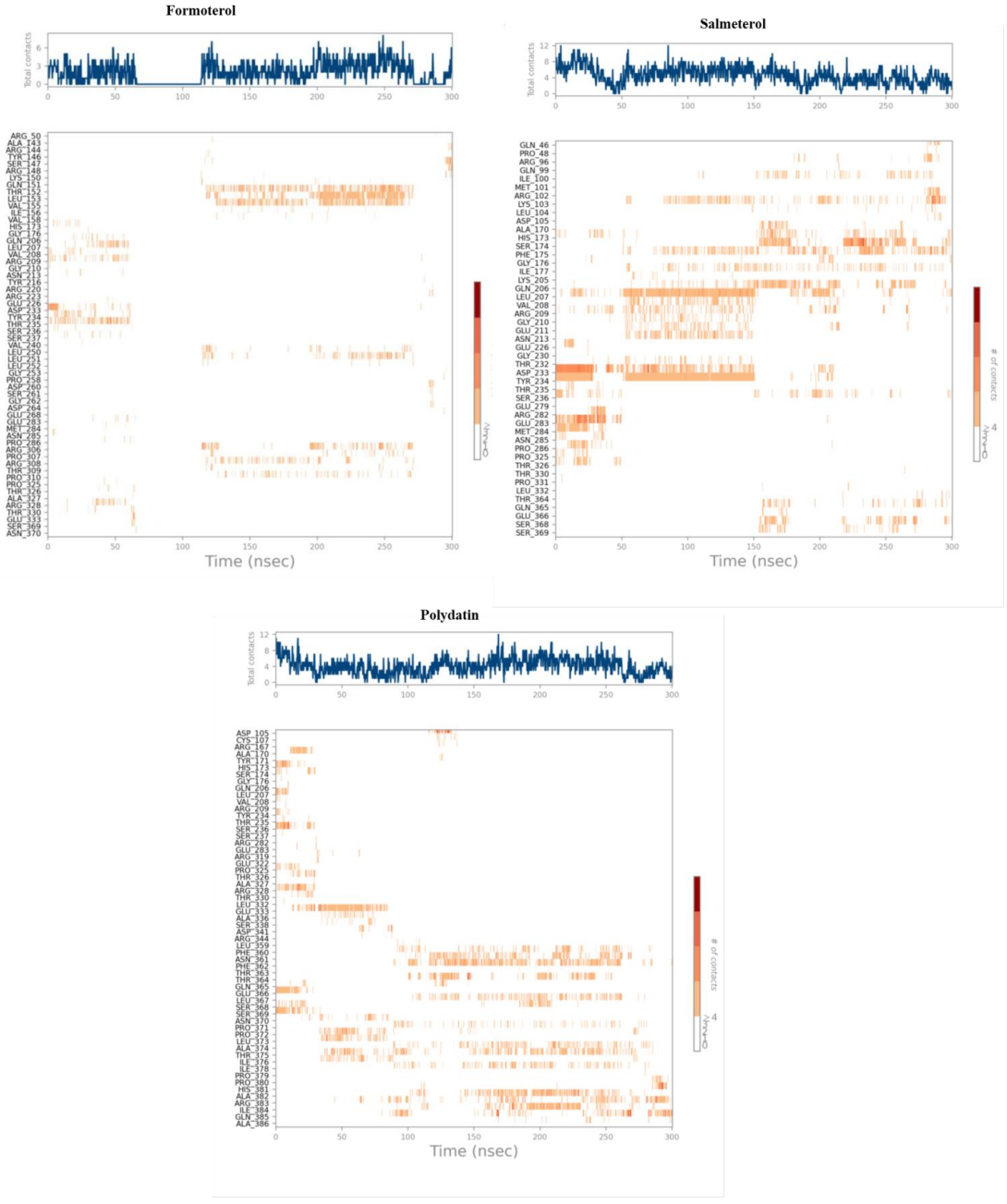

Figure 3: Illustrating the timeline of Protein-Ligand Contacts with several interacting residues

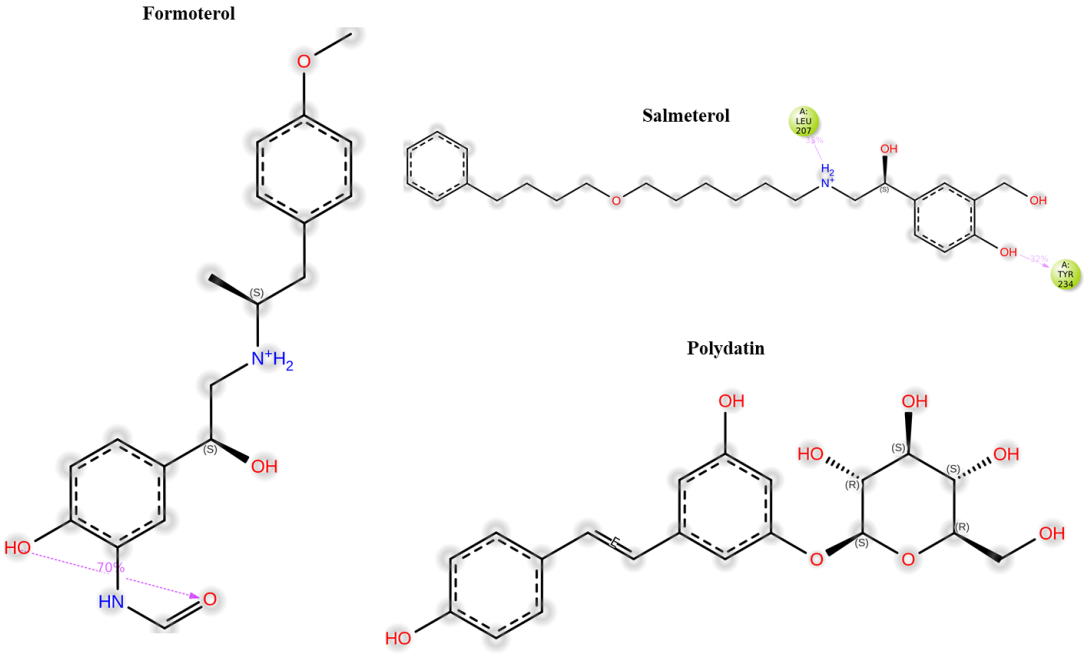

Figure 4: Protein-Ligand contact interaction with amino acid residues during Molecular dynamics simulation

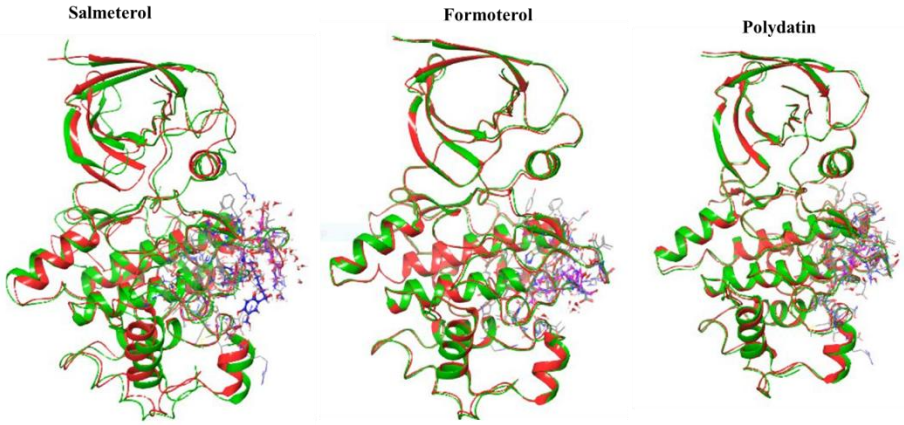

Figure 5: Superimposed protein structures of before dynamics (IFD structure ribbon in red colour and ligand in blue) and post dynamics (MD structure ribbon in green colour and ligand in magenta).

Figure 5 caption: Before and after the MD analysis the RMSD of the protein was minimal and within the acceptable range.

Analysis of RMSD fluctuations and Ligand interaction with amino acid residues of Protein during MD simulation studies

During MD simulations, GSK-3β **(1PYX-protein)** & ligand **(Formoterol)** binding stability were examined through RMSD variations during Molecular Dynamics simulations. The RMSD fluctuations were assessed independently for the protein and ligand structures in the MD simulations, and they all fell within the 3Å range. Then that complex was regarded as stable. During the simulation, the intermolecular contact between protein and ligand was examined based on durability. Then, throughout the MD simulations, the analysis for the RMSD plot was mentioned separately for conformation of protein in the entire trajectory of molecular dynamic simulation study. The RMSD fluctuation for the protein was initially noticed at 1.8Å and spike to 2.2Å was noticed at 100ns. After 100ns a slight raise in spike was noticed at 2.3Å. The episodes of decrease and increase RMSD was observed from 120 ns to 210 ns and after 210 ns the spike was raised to 2.5 Å. The episodes of decrease and increase RMSD was observed from 210 ns to 280 ns and a slight decrease in spike was noticed at 300ns.

The RMSD fluctuations for the ligand (**Formoterol)** were initially noticed at 38 Å and spiked to 74 Å at 100ns and fluctuations were constant still 250ns, then after 250ns the spike was raised to 80 Å. Then episodes of raise and fall in RMSD was observed between 270 ns and 300 ns from 16 Å to 44 Å.

During MD simulations, the protein **(1PYX)** & ligand **(Salmeterol)** binding stability were examined through RMSD variations during Molecular Dynamics simulations. The RMSD fluctuation for the protein was initially noticed at 0.5 Å and spikes to 4 Å at 80 ns. The episodes of raise and fall in protein RMSD was noticed from 2 Å to 3.5 Å between 80 ns and 180 ns. The episodes of raise and fall in protein RMSD was noticed from 1.8 Å to 2.3Å between 180ns and 300ns.

The ligand **(Salmeterol)** RMSD was initiated at 0Å and spikes to 12Å. The episodes of raise and fall in ligand RMSD was noticed from 80ns and 150ns. A slight decrease in ligand RMSD was observed at 11Å and a slight increase in ligand RMSD was noticed at 21Å. After 200 ns the ligand RMSD was noticed at 24 Å. The episodes of raise and fall in protein RMSD was noticed from 13Å to 18Å between 201ns and 300ns.

During MD simulations, the protein (**1PYX**) & ligand **(Polydatin)** binding stability were examined through RMSD variations during Molecular Dynamics simulations. The RMSD fluctuation for the protein was initially noticed at 0Å and spikes to 2.9Å. The episodes of raise and fall in RMSD of protein was noticed from 1.7Å to 2.6Å between 81ns and 180ns. Then gradual increase in spike was noticed at 2.8Å and the episodes of raise and fall in RMSD of protein was noticed from 3.5Å to 2.3Å between 200ns and 250ns. After 250ns a slight increase in RMSD was noticed at 2.4Å and the episodes of raise and fall in RMSD of protein was noticed from 1.7Å to 2.6Å between 81ns and 180ns. The episodes of raise and fall in RMSD of protein was noticed from 2.1 Å to 3.1Å between 181ns and 300ns.

The ligand **(Polydatin)** RMSD fluctuation was initiated at 0Å and at 100ns the RMSD spike was noticed at 26Å. After 100ns the spike was noticed at 30Å. Equilibrium plateau was spotted from 20Å to 24Å between 110ns and 260ns. After 260 ns a slight increase in RMSD spike was noticed at 34 Å. A slight decrease in RMSD spike was noticed and Spike RMSD was noticed at 39 Å when it reached to 300ns.

There is no interactions for 300ns while it has interactions for 100ns. Even most of the structural changes and stability of the complex was good for 100ns compared with 300ns.

CONCLUSION

GSK-3β is involved in various physiological pathways i.e. cell cycle development, metabolism, and neuroprotection, and an elevated activity and expression

of GSK-3β is reported in Alzheimer's disease. In the present study, we have used in-silico docking studies for FDA-approved ligands against GSK-3β (PDB ID: 1PYX) protein. Among selected hit molecules, Salmeterol showed the most stable interactions with these key amino acid residues and to validate these findings very strongly further in-vitro and in-vivo experimental studies are required to conform the findings.

ACKNOWLEDGMENT

The authors would like to thank the Indian Council of Medical Research, New Delhi, India for ICMR-SRF (3/1/2/172/Neuro/2021-NCD-I) to Suggala Ramya Shri.

Funding: 3/1/2/172/Neuro/2021-NCD-I

Authorship contribution statement

Suggala Ramya Shri: Study Concept or Design, Data Collection, Data Analysis or Interpretation, Writing the Paper; **Yogendra Nayak**: Reviewing, Mentoring; **K Sreedhara Ranganath Pai:** Study Concept or Design, Data Analysis or Interpretation, Writing the Paper.

Data Availability: The data generated during the whole study are included in this article and will be available on request from the corresponding author.

Declarations

In this research, we have used a large number of molecular docking software for shortlisting the compounds of interest.

Competing interest: The authors declare that they were no conflicts of interest.

REFERENCES

1. Bomasang-Layno E, Bronsther R. Diagnosis and Treatment of Alzheimer's Disease: An Update. Delaware J Public Heal. 2021;7(4).
2. Valencia E. FireScholars ELUCIDATING THE ROLE OF O-GLCNACYLATION AND GSK3B IN ALZHEIMER ' S DISEASE. 2022;
3. Ugbaja SC, Lawal IA, Abubakar BH, Mushebenge AG, Lawal MM, Kumalo HM. Allostery Inhibition of BACE1 by Psychotic and Meroterpenoid Drugs in Alzheimer's Disease Therapy. Molecules. 2022;27(14).
4. Bradley D, Beltrao P. Evolution of protein kinase substrate recognition at the active site. PLoS Biol. 2019;17(6):1–25.
5. Sunkari YK, Meijer L, Flajolet M. The protein kinase CK1: Inhibition, activation, and possible allosteric modulation. Front Mol Biosci. 2022;9(August):1–10.
6. Martinez A, Castro A, Dorronsoro I, Alonso M. Glycogen synthase kinase 3 (GSK-3) inhibitors as new promising drugs for diabetes, neurodegeneration, cancer, and inflammation. Med Res Rev. 2002;22(4):373–84.
7. Wei J, Wang J, Zhang J, Yang J, Wang G, Wang Y. Development of inhibitors targeting glycogen synthase kinase-3β for human diseases: Strategies to improve selectivity. Eur J Med Chem [Internet]. 2022;236:114301. Available from: https://doi.org/10.1016/j.ejmech.2022.114301
8. Pandey MK, DeGrado TR. Glycogen synthase kinase-3 (GSK-3)-targeted therapy and imaging [Internet]. Vol. 6, Theranostics. Ivyspring International Publisher; 2016 [cited 2021 Apr 14]. p. 571–93. Available from: /pmc/articles/PMC4775866/
9. Di Fruscia P, Edfeldt F, Shamovsky I, Collie GW, Aagaard A, Barlind L, et al. Fragment-Based Discovery of Novel Allosteric MEK1 Binders. ACS Med Chem Lett. 2021;12(2):302–8.
10. Balboni B, Tripathi SK, Veronesi M, Russo D, Penna I, Giabbai B, et al. Identification of Novel GSK-3β Hits Using Competitive Biophysical Assays. Int J Mol Sci. 2022;23(7).
11. Lu X, Smaill JB, Ding K. New Promise and Opportunities for Allosteric Kinase Inhibitors. Angew Chemie - Int Ed. 2020;59(33):13764–76.

12. Morales-Garcia JA, Luna-Medina R, Alonso-Gil S, Sanz-Sancristobal M, Palomo V, Gil C, et al. Glycogen synthase kinase 3 inhibition promotes adult hippocampal neurogenesis in vitro and in vivo. ACS Chem Neurosci. 2012;3(11):963–71.
13. Martínez-González L, Gonzalo-Consuegra C, Gómez-Almería M, Porras G, de Lago E, Martín-Requero Á, et al. Tideglusib, a non-atp competitive inhibitor of gsk-3as a drug candidate for the treatment of amyotrophic lateral sclerosis. Int J Mol Sci. 2021;22(16).
14. Rico A, Guembelzu G, Palomo V, Martínez A, Aiastui A, Casas-fraile L, et al. Allosteric modulation of GSK-3β as a new therapeutic approach in limb girdle muscular dystrophy R1 Calpain 3-related. Int J Mol Sci. 2021;22(14):1–18.
15. Bertrand JA, Thieffine S, Vulpetti A, Cristiani C, Valsasina B, Knapp S, et al. Structural characterization of the GSK-3β active site using selective and non-selective ATP-mimetic inhibitors. J Mol Biol [Internet]. 2003 Oct 17 [cited 2021 Apr 30];333(2):393–407. Available from: https://pubmed.ncbi.nlm.nih.gov/14529625/
16. Satarker S, Maity S, Mudgal J, Nampoothiri M. In silico screening of neurokinin receptor antagonists as a therapeutic strategy for neuroinflammation in Alzheimer's disease. Mol Divers [Internet]. 2022;26(1):443–66. Available from: https://doi.org/10.1007/s11030-021-10276-6
17. Chauhan N, Gajjar A. Classifying druggability on potential binding sites of glycogen synthase kinase-3β: An in-silico assessment. Acta Pharm Sci. 2017;55(3):43–60.
18. Palomo V, Soteras I, Perez DI, Perez C, Gil C, Campillo NE, et al. Exploring the binding sites of glycogen synthase kinase 3. identification and characterization of allosteric modulation cavities. J Med Chem. 2011;54(24):8461–70.
19. Ter Haar E, Coll JT, Austen DA, Hsiao HM, Swenson L, Jain J. Structure of GSK3β reveals a primed phosphorylation mechanism. Nat Struct Biol [Internet]. 2001 [cited 2021 Apr 14];8(7):593–6. Available from: https://pubmed.ncbi.nlm.nih.gov/11427888/
20. Silva GM, Borges RS, Santos KLB, Federico LB, Francischini IAG, Gomes SQ, et al. Revisiting the Proposition of Binding Pockets and Bioactive Poses for GSK-3β Allosteric Modulators Addressed to Neurodegenerative Diseases. Int J Mol Sci [Internet]. 2021 Jul 31;22(15):8252. Available from: https://www.mdpi.com/1422-0067/22/15/8252
21. Palomo V, Soteras I, Perez DI, Perez C, Gil C, Campillo NE, et al. Exploring the Binding Sites of Glycogen Synthase Kinase 3. Identification and Characterization of Allosteric Modulation Cavities. J Med Chem [Internet]. 2011 Dec 22;54(24):8461–70. Available from: https://pubs.acs.org/doi/10.1021/jm200996g
22. Madhavi Sastry G, Adzhigirey M, Day T, Annabhimoju R, Sherman W. Protein and ligand preparation: Parameters, protocols, and influence on virtual screening enrichments. J Comput Aided Mol Des. 2013;27(3):221–34.
23. Bowers KJ, Chow E, Xu H, Dror RO, Eastwood MP, Gregersen BA, et al. Scalable algorithms for molecular dynamics simulations on commodity clusters. Proc 2006 ACM/IEEE Conf Supercomput SC'06. 2006;(November).
24. Mangala K, Vinayak W, Aasiya C, Chandrakant B, Amol M, Kumar D, et al. Reconnoitering imidazopyridazines as anticancer agents based on virtual modelling approach: quantitative structure activity relationship, molecular docking and molecular dynamics. J Biomol Struct Dyn [Internet]. 2023;0(0):1–18. Available from: https://doi.org/10.1080/07391102.2023.2204502
25. Buch I, Fishelovitch D, London N, Raveh B, Wolfson HJ, Nussinov R. Allosteric regulation of glycogen synthase kinase 3β: A theoretical study. Biochemistry. 2010;49(51):10890–901.
26. Silva GM, Alves VM, Gomes SQ, Hochuli JE, Muratov

E, Tropsha A, et al. Discovery of Potential GSK- 3β Allosteric Modulators for Alzheimer's Disease Guilherme Martins Silva. ChemRxiv. 2023;1–30.

27. Alzyoud L, Bryce RA, Al Sorkhy M, Atatreh N, Ghattas MA. Structure-based assessment and druggability classification of protein–protein interaction sites. Sci Rep [Internet]. 2022;12(1):1–18. Available from: https://doi.org/10.1038/s41598-022-12105-8
28. Palomo V, Soteras I, Perez DI, Perez C, Gil C, Campillo NE, et al. Exploring the binding sites of glycogen synthase kinase 3. identification and characterization of allosteric modulation cavities. J Med Chem [Internet]. 2011 Dec 22 [cited 2021 Apr 30];54(24):8461–70. Available from: https://pubs.acs.org/doi/abs/10.1021/jm200996g
29. Tolosa E, Litvan I, Höglinger GU, Burn DJ, Lees A, Andrés M V., et al. A phase 2 trial of the GSK-3 inhibitor tideglusib in progressive supranuclear palsy. Mov Disord. 2014;29(4):470–8.
30. Höglinger GU, Huppertz HJ, Wagenpfeil S, Andrés M V., Belloch V, León T, et al. Tideglusib reduces progression of brain atrophy in progressive supranuclear palsy in a randomized trial. Mov Disord. 2014;29(4):479–87.
31. Zhang P, Li S, Gao Y, Lu W, Huang K, Ye D, et al. Novel benzothiazinones (BTOs) as allosteric modulator or substrate competitive inhibitor of glycogen synthase kinase 3β (GSK-3β) with cellular activity of promoting glucose uptake. Bioorg Med Chem Lett [Internet]. 2014 Dec;24(24):5639–43. Available from: https://linkinghub.elsevier.com/retrieve/pii/S0960894X14011494
32. Zhang P, Hu HR, Bian SH, Huang ZH, Chu Y, Ye DY. Design, synthesis and biological evaluation of benzothiazepinones (BTZs) as novel non-ATP competitive inhibitors of glycogen synthase kinase-3β (GSK-3β). Eur J Med Chem [Internet]. 2013;61:95–103. Available from: http://dx.doi.org/10.1016/j.ejmech.2012.09.021
33. Palomo V, Perez DI, Roca C, Anderson C, Rodríguez-Muela N, Perez C, et al. Subtly Modulating Glycogen Synthase Kinase 3 β: Allosteric Inhibitor Development and Their Potential for the Treatment of Chronic Diseases. J Med Chem. 2017;60(12):4983–5001.

دراسات الإرساء الجزيئي والمحاكاة للأدوية المعتمدة من إدارة الغذاء والدواء الأمريكية (FDA) المستهدِفة للتثبيط الألوستيري لإنزيم كيناز جليكوجين سينثاز−3 بيتا (GSK-3β)

سوغالا راميا شري[1]، يوجيندرا نايك[1]، ك. سريدهارا رانغاناث باي[1]*

[1] قسم علم الأدوية، كلية مانيبال للعلوم الصيدلانية، أكاديمية مانيبال للتعليم العالي (MAHE)، مانيبال 576104، الهند.

ملخص

الخلفية :أصبح تثبيط إنزيم كيناز جليكوجين سينثاز−3 بيتا (GSK-3β) بآليات تثبيط مختلفة هدفًا دوائيًا مهمًا لعلاج الأمراض التنكسية العصبية مثل مرض ألزهايمر .(AD) يتميز مرض ألزهايمر باضطرابات في الإدراك وفقدان الذاكرة والتغيرات السلوكية. وتتمثل العلامات المرضية المميزة للمرض، والتي تظهر قبل الأعراض السريرية، في التشابكات الليفية العصبية (Neurofibrillary tangles) ولويحات الأميلويد.(Amyloid plaques)

الهدف والأهداف :ركزت هذه الدراسة على منهج تنبؤي قائم على المحاكاة الحاسوبية (in silico) لإجراء فحص افتراضي لليغاندات المعتمدة من إدارة الغذاء والدواء الأمريكية) قاعدة بيانات(DrugBank ، بهدف استهداف الجيب الألوستيري لإنزيمGSK-3β ، وذلك باستخدام برنامج شرودنغر (Schrödinger) عبر واجهة.Maestro

النتائج والاستنتاج :بعد تنفيذ عدة مراحل من تصفية المركبات، ومن بين 2133 ليغاندًا معتمدًا من FDA، تم اختيار ثلاثة مركبات فقط — فورموتيرول (Formoterol)، سالمتيرول (Salmeterol)، وبوليداتين — (Polydatin)لإجراء الإرساء المتوافق المحفَّز .(Induced Fit Docking, IFD)وبعد تطبيق تقنية IFD، تم اقتراح أفضل وضعية ارتباط (Top Pose) لكل من المركبات الثلاثة لإجراء دراسات الديناميكا الجزيئية باستخدام وحدة .Desmondأظهر مركب الفورموتيرول أكثر التفاعلات استقرارًا مع بقايا الأحماض الأمينية الرئيسية في الموقع الفعال. ومع ذلك، فإن تأكيد هذه النتائج يتطلب إجراء دراسات تجريبية لاحقة.

الكلمات الدالة: مرض ألزهايمر؛ كيناز جليكوجين سينثاز−3 بيتا (GSK-3β)؛ الإرساء الجزي.

* ***المؤلف المراسل: ك. سريدَهارا رانغاناث باي***

ksr.pai@manipal.edu

تاريخ استلام البحث 2024/7/4 وتاريخ قبوله للنشر 2025/2/20.